ARCHIVES OF ACOUSTICS
Vol. **46**, No. 2, pp. 197–204 (2021)
DOI: 10.24425/aoa.2021.136575

Research Paper

Revisiting the Open-End Reflection Coefficient and Turbulent Losses in an Organ Pipe with Low Mach Number Flow

Viktor HRUŠKA*, Pavel DLASK

Academy of Performing Arts in Prague
Musical Acoustics Research Centre
Prague, Czech Republic
*Corresponding Author e-mail: hruska.viktor@hamu.cz

(*received April 28, 2020; accepted December 28, 2020*)

The reflection coefficient of the open end belongs among the essential parameters in the physical description of a flue organ pipe. It leads directly to practical topics such as the pipe scaling. In this article, sound propagation is investigated inside an organ pipe with the most intense mean flow that is achievable under musically relevant conditions. A theoretical model is tested against the experimental data to obtain a suitable formula for the reflection coefficient when a non-negligible flow through the open end is considered. The velocity profile is examined by means of particle image velocimetry. A fully developed turbulent profile is found and interactions of the acoustic boundary layer with the turbulent internal flow are discussed. A higher value of the end correction than expected from the classical result of Levine and Schwinger is found, but this feature shall be associated with the pipe wall thickness rather than the mean flow effects.

Keywords: organ pipe; reflection coefficient; end correction; flow-acoustic interactions.

1. Introduction

Voicing of a flue organ pipe is a sensitive process with many features that are not fully understood from the physical point of view. The main reason behind it lies in the inherent nonlinearity of the complex flow-acoustic interactions within the mouth region (see Fig. 1 for a simplified scheme). For the same reason, it is not very reliable to assess fine details of the radiated sound from the crude voicing parameters, such as cut-up width, foot, or windchest pressure. The far-field sound is a nontrivial composition of the sound radiated from the mouth and the open end. In order to bypass these "black boxes", the aeroacoustics of the pipe mouth is entirely put aside and more direct measurements and theoretical considerations are dedicated to the processes "outside the black box". Namely, our focus is on the flow at the pipe's open-end and connected changes in the reflection coefficient, end correction and damping. All the mentioned can be investigated inside the region where the linear sound propagation can be assumed. The significance of the study for organ building is apparent since much of the mentioned (e.g. the flow field at the open end) have not been directly measured and discussed for this particular purpose yet.

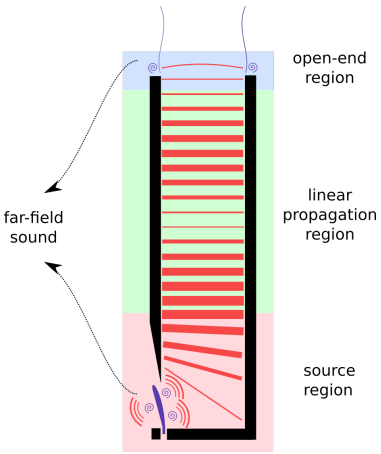

Fig. 1. A simplified scheme of sound propagation regions of an open flue organ pipe.

The main goal of this article is to discuss the theoretical predictions for the above-mentioned quantities and provide their experimental verification. In order to investigate the mean flow effects, an experimental organ pipe is loaded with the highest input (foot) pressure under which it still produces musically relevant sound.

The paper is organized as follows. This introduction is followed by Sec. 2 (Theory) which sums up the description of the flow-acoustic conditions by nondimensional numbers and for clarity, and it is further divided into subsections dealing with the theoretical predictions regarding the flow turbulence (Subsec. 2.1), the reflection coefficient and the end correction (Subsec. 2.2) and finally, some remarks are given to the determination of the quasi-plane wave amplitudes from the experimental data (Subsec. 2.3). The measurement setup is introduced in Sec. 3, followed by the results (Sec. 4) of the hydrodynamic and acoustic measurements on the representative case of a transparent organ pipe. Some interesting points connected to the results and quantities not measured in this study are addressed in the Discussion (Sec. 5). The conclusions are finally given in Sec. 6.

2. Theory

First, let us introduce nondimensional characteristic numbers describing the situation inside the pipe and at its open end. The ratio of the velocity inside the pipe U_0 to the sound speed c_0 is the Mach number $\mathrm{M} = U_0/c_0$. The reference velocity U_0 is taken as the centerline velocity of the jet at the open end. The reader should refer to the discussion in (Hirschberg, Hoeijmakers, 2014) regarding the differences between the centerline and mean velocity for this purpose. The Reynolds number relating the inertial and viscous forces is defined here as $\mathrm{Re} = 2aU_0/\nu$ with a, ν denoting the pipe radius and kinematic viscosity respectively. The Helmholtz number is introduced in the usual manner as $ka = \omega a/c_0$, with k, ω being the wavenumber and the angular frequency, respectively. Strouhal number is defined for our case as $\mathrm{Sr} = ka/\mathrm{M}$. The list of the nondimensional numbers is completed with the Prandtl number, the ratio of viscous and thermal effects on the momentum diffusion, which is given for air under normal conditions as $\mathrm{Pr} = 0.71$. Whenever the pipe radius is needed, even though the pipe cross-section is rectangular, the effective value of $a = \sqrt{S/\pi}$ is employed, where S is the cross-sectional area.

Our considerations are limited to the quasi-plane wave propagation, which corresponds to a frequency range $ka < 1.84$ (a value of the first zero of the first-order Bessel function derivative). Usually, all musically important frequencies lie within this region. On the other hand, $ka \sim 1$ is quite common, so the widely used low-frequency approximation cannot be blindly employed. It is reasonable to assume that the mean flow through the pipe is of the low Mach number, and hence the high Strouhal number limit is justified. Physically, it means that the alternating flow primarily governs the dynamics at the open end. However, it would be doubtful to exclude the mean flow effects a priori. The following text aims precisely at such questions.

In the following, we assume the time-harmonic behaviour of the acoustic pressure and acoustic quantities in general. Together with the quasi-plane waves assumption, we can express the acoustic pressure as

$$\widehat{p}(x,f) = \widehat{P}_+(f)e^{-\mathrm{i}\Gamma_+ x} + \widehat{P}_-(f)e^{\mathrm{i}\Gamma_- x}, \tag{1}$$

where f, $\Gamma_\pm$, P_+, P_- denote the frequency, the complex wavenumber discussed below and the amplitudes of forward and backward propagating waves, respectively. The waves are propagating along the x axis oriented from the pipe interior outwards. Consequently, the transversal coordinate (see e.g. Fig. 3) is denoted y throughout the article. The complex pressure reflection coefficient of the open end is then defined as $R = \widehat{P}_-/\widehat{P}_+$.

2.1. Turbulent flow inside the pipe and the complex wavenumber

Assuming the mean flow velocities around 1 m/s and pipe radii in centimeters, many internal pipe flows are within the range of Reynolds numbers suggesting the transition or turbulent flow (for further commentary see e.g. (Schlichting, Gersten, 2016)). The question is whether this estimate of the pipe flow condition is applicable to the case of an organ pipe in general and whether the organ pipe is long enough for the turbulent flow profile to develop. As it is confirmed below experimentally, there are cases in which the turbulence occurring in the pipe mouth region does not relaminarize and the flow profile typical for developed turbulence is observable near the open end. Therefore, we proceed with the considerations with the assumption of this kind of behaviour.

As it was pointed out (Weng *et al.*, 2013; Peters *et al.*, 1993), of the key importance is the ratio of the acoustic boundary layer thickness, $\delta_{\mathrm{ac}} = \sqrt{2\nu/\omega}$, to the laminar viscous sublayer of the mean flow profile, δ_{visc}. For a rough approximation, we make use of the law of the wall and the flat plate approximation (cf. e.g. (Lautrup, 2011)) with subsequent experimental verification. The dimensionless wall distance, $y^+ \approx 5$, corresponds to the dimensional viscous sublayer thickness, $\delta_{\mathrm{visc}} = 1$ mm, given that the boundary layer is at least 0.1 m long and the freestream velocity is ca. 1 m/s (see Fig. 5 for experimental confirmation). It follows that the acoustic boundary layer lies within the viscous sublayer for all frequencies in the audio range. Therefore, we shall neglect the interactions of the acoustic boundary layer velocities with the eddy viscosity (see the discussion in (Weng *et al.*, 2013)).

The complex wavenumber is defined as

$$\Gamma_\pm = \frac{k - \mathrm{i}\alpha_\pm}{1 \pm \mathrm{M}}, \tag{2}$$

where $\alpha_\pm$ are damping coefficients for the downstream and upstream propagating wave. In our range of Mach

numbers, we can neglect this distinction (see the Discussion) and put $\alpha_+ \approx \alpha_- \approx \alpha_0$, with α_0 being the damping coefficient for a viscous, thermally conductive, quiescent fluid with no-slip and isothermal condition for the acoustic perturbations at the wall. For an ideal gas, it can be expressed (Blackstock, 2000):

$$\alpha_0 = \frac{1}{a}\sqrt{\frac{\omega\nu}{2c_0^2}}\left(1+\frac{\gamma-1}{\mathrm{Pr}}\right), \tag{3}$$

where γ is the ratio of the specific heats.

2.2. Reflection coefficient and end correction

The reflection coefficient may be expressed in terms of an additional distance ℓ that the wave must travel to the point of phase inversion, $R = -|R|\exp(2\mathrm{i}\Gamma\ell)$, where $\Gamma = (\Gamma_+ + \Gamma_-)/2$. The distance ℓ is known as the end correction and can be calculated by rearranging the last expression:

$$\ell = \frac{1}{2\mathrm{i}\Gamma}\ln\left(-\frac{R}{|R|}\right). \tag{4}$$

A modern history of the theoretical effort to obtain the reflection coefficient and the end correction of an unflanged circular pipe begins with the classical work of Levine and Schwinger (1948). Munt (1990) extended their work by the effects of the nonzero mean flow. The work relies on the Wiener-Hopf method and unfortunately requires numerical evaluation at some points of the solution. Simpler expressions were found by Cargill (1982) in the low Mach and the low Helmholtz number limit and by Rienstra (1983) in the low Strouhal number limit. However, as we have already mentioned, the condition $ka \to 0$ does not necessarily hold in our case and an opposite limit would be needed in the Strouhal number. Instead, we employ an expression derived by Hirschberg and Hoeijmakers (2014) making use of the vortex sound theory. Assuming that the temperature inside the pipe is the same as the ambient one, the equation reads:

$$\begin{aligned}|R| &= \frac{4-(ka)^2+4\mathrm{M}(\mathrm{M}+1)}{(ka)^2+4\mathrm{M}+4\sqrt{\mathrm{M}(ka)^2+(\mathrm{M}^2+1)^2}}\\ &\approx \frac{16+(2\mathrm{M}-1)(ka)^4}{\left[(ka)^2+4\right]^2},\end{aligned} \tag{5}$$

where the terms of $\mathcal{O}\left(\mathrm{M}^2\right)$ and higher were neglected in the last expression. Although it is formally derived with the assumption $ka < 1$, the relation is shown below to be sufficiently corresponding to the experimental data even for Helmholtz number slightly exceeding 1.

The end correction value $\ell \approx 0.61a$, originally due to Levine and Schwinger, has been adopted in many articles and textbooks, e.g. the classic book of Fletcher and Rossing (1998) to name one. This expression holds for a thin-walled tube without flow. The analysis of Rienstra (1983) shows that the end correction can be significantly smaller in the low Strouhal number limit, which is not the typical case for an organ pipe. On the other hand, the value of Levine and Schwinger is again reached for the high Strouhal numbers. Cargill (1982) stated that for the intermediate range of Strouhal numbers there is no approximate expression for the end correction. Apart from that, Ando (1969) found out that the end correction increases with the pipe thickness towards the value for a pipe termination in an infinite flange ($\ell/a = 0.82$, as calculated by Nomura *et al.* (1960). Hence, the question for experimental investigation arises: does the organ pipe wall thickness outweigh the flow effects at least at the fundamental frequency, i.e. for the lowest Strouhal number?

For the sake of completeness, we shall mention that, apart from the analytical predictions, there are fine articles dealing with these problems by means of numerical simulations (see e.g., (da Silva, Greco, 2019)) even within the realm of the physics of musical instruments (e.g., (da Silva *et al.*, 2010)). However, it is not necessary to go in detail with this approach as the already given analytical predictions are sufficient for the results given below.

2.3. Determination of the $\widehat{P}_+$, $\widehat{P}_-$ amplitudes

When the acoustic pressure is known at multiple locations, $\widehat{p}(x_1,f), \widehat{p}(x_2,f), ..., \widehat{p}(x_n,f)$, we may use Eq. (1) to form the set of linear equations:

$$\mathbf{A}\cdot\mathbf{p} = \mathbf{b}, \tag{6}$$

with

$$\mathbf{A} = \begin{bmatrix} e^{-\mathrm{i}\Gamma x_1} & e^{\mathrm{i}\Gamma x_1} \\ e^{-\mathrm{i}\Gamma x_2} & e^{\mathrm{i}\Gamma x_2} \\ \vdots & \vdots \\ e^{-\mathrm{i}\Gamma x_n} & e^{\mathrm{i}\Gamma x_n} \end{bmatrix}, \qquad \mathbf{p} = \begin{bmatrix} \widehat{P}_+(f) \\ \widehat{P}_-(f) \end{bmatrix},$$
$$\mathbf{b} = \begin{bmatrix} \widehat{p}(x_1,f) \\ \widehat{p}(x_2,f) \\ \vdots \\ \widehat{p}(x_n,f) \end{bmatrix}. \tag{7}$$

The set in Eq. (6) is overdetermined. Therefore, the Moore-Penrose pseudoinverse $(\ )^+$ is employed. In other words, the complex amplitudes are obtained by means of the least-squares fitting.

3. Measurement setup

A transparent flue organ pipe with a fundamental frequency of 210 Hz was used for experiments. The ef-

fective open-end radius was $a = 28$ mm, the wall thickness of 7 mm corresponds to the wooden organ pipes. From the particle image velocimetry measurements, we determined the freestream velocity inside the pipe and right above it as $U = 1.6$ m/s. That leads to the Mach number $\mathrm{M} \approx 0.005$, the Strouhal number at the fundamental frequency, $\mathrm{Sr} \approx 23$, and the Reynolds number, $\mathrm{Re} \approx 6000$.

The windchest pressure was 900 Pa, the cut-up of 14 mm and the flue width 1.4 mm. The flue was situated slightly inside the pipe, ca. 2 mm to the interior regarding the labium plane.

The particle image velocimetry is a standard technique nowadays, so for brevity, we are not going into details. The reader should refer to Raffel *et al.* (2007) for a general description and might be further interested in PIV measurements in organ pipes and associated data processing techniques, as delineated in (Yoshikawa *et al.*, 2012; Mickiewicz, 2015; Hruška, Dlask, 2017; 2019a).

A detailed description and discussion of the spatial pressure waveform measurement may be found in our previous work (Hruška *et al.*, 2019). A thin (0.3% of the pipe's cross-section) sensitive pressure probe was lowered along the pipe centerline. Its signal was synchronized with a small reference microphone placed at the half of the pipe height, thus effectively emulating the multiple microphone method (cf., e.g., (Jang, Ih, 1998), see Fig. 2 for schematics). The pressure was measured at 19 positions spanning from $x = -0.57$ m to $x = -0.03$ m (0 at the open end).

In order to assure that the measurements take place in the quasi-plane wave propagation region, numerical simulations of the pressure distribution at the pipe's eigenfrequencies were made. For the sake of simplicity, the eigenvalue problem for the Helmholtz equation $\nabla^2 p + (\omega^2/c_0^2)p = 0$ was considered. Both the mouth and the open end were assumed the ideal pressure release surfaces. Results of the lowest and the highest eigenfrequencies considered below are depicted in Fig. 3. For clarity, only a planar cross-section is given, but the whole 3D computation was carried on. It follows that the measurement positions are safely outside the region of the wavefront deflection. Note, however, that in some regions of the pipe interior the wavefronts exhibits a nonzero curvature even for low frequencies. Hence, the use of the term quasi-plane wave throughout the article.

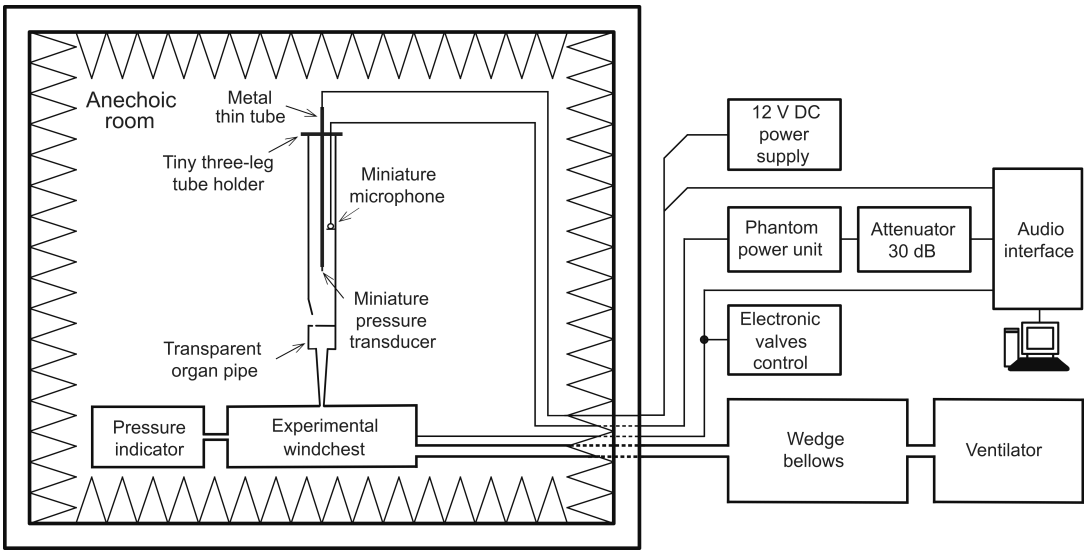

Fig. 2. Schematics of the internal acoustic pressure measurement.

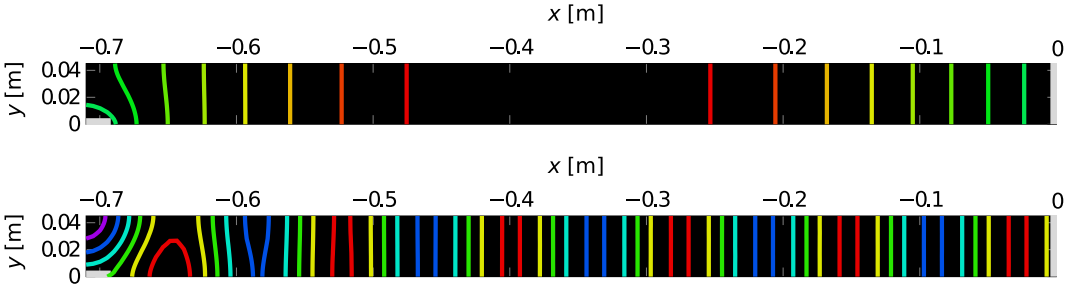

Fig. 3. Isolines of the acoustic pressure in the lowest eigenmode (up) and the last eigenmode before the transversal patterns occur (down). The mouth and the open end are marked in grey.

4. Results

Figures 4, 5, and 6 depict the results of the PIV measurement at the open end. From the mean flow measurement, it is clear that the flow separation occurs, and a free jet is formed. The mean flow profile taken inside the pipe exihibits the shape typical for turbulent flows. It follows from the fit in Fig. 5 that the viscous sublayer thickness is ca. 2 mm. That is more than the reserved assessment given above, but it only supports the claim that the acoustic boundary layer is fully immersed in the laminar viscous sublayer of the flow profile.

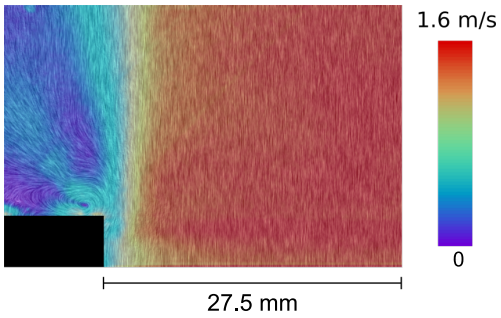

Fig. 4. Visualization of the mean flow at the open end (detail of the flow separation) by the line integral convolution. A half-width of the jet is depicted.

As expected from the Strouhal number value, the instabilities are strong enough to revert the flow direction in some phases. Examples of the instantaneous flow field are given in Fig. 6. A flow stagnation point is formed above the pipe in some phase angles and inward suction at the pipe edges is observed (Fig. 6c). A tiny recirculation zone is created at the pipe's edge (see Fig. 4), but besides that, no major perturbations of the shear layer, such as convection of developed vortices, has been observed. That is in accordance with the evaluation of the reflection coefficient given below, which does not exhibit traits of significant flow-acoustic interactions.

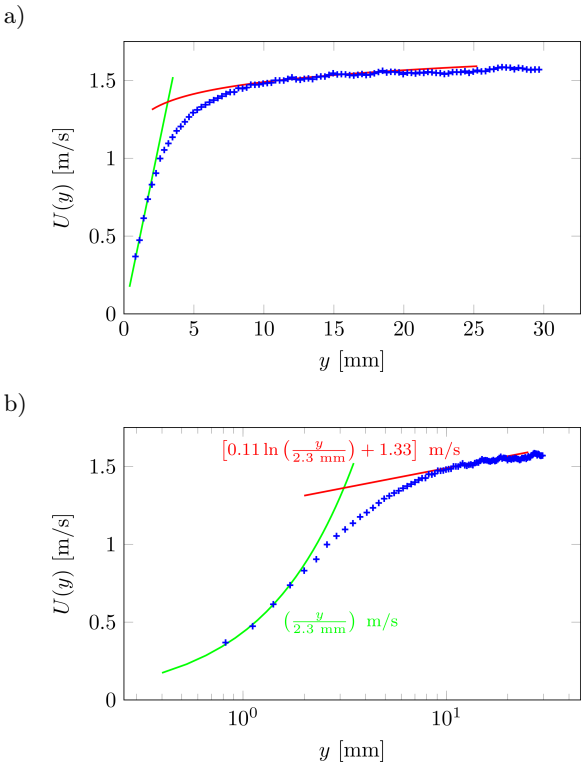

Fig. 5. Half profile of the flow inside the pipe 10 mm below the open end: a) linear scale, b) logarithmic abscissa with the fit parameters.

Results of the reflection coefficient and the end correction calculations are shown in Fig. 7. The experimental data points correspond to the pipe harmonics. Otherwise, the spectral components are so weak and uncertain that obviously meaningless expressions tending to 0/0 are found during the data processing. The theoretical prediction based on Eq. (5) matches the experimental results very well.

On the contrary, the end correction is higher than the value $\ell/a = 0.61$. It follows that the wall thickness is the major influence, and the end correction around

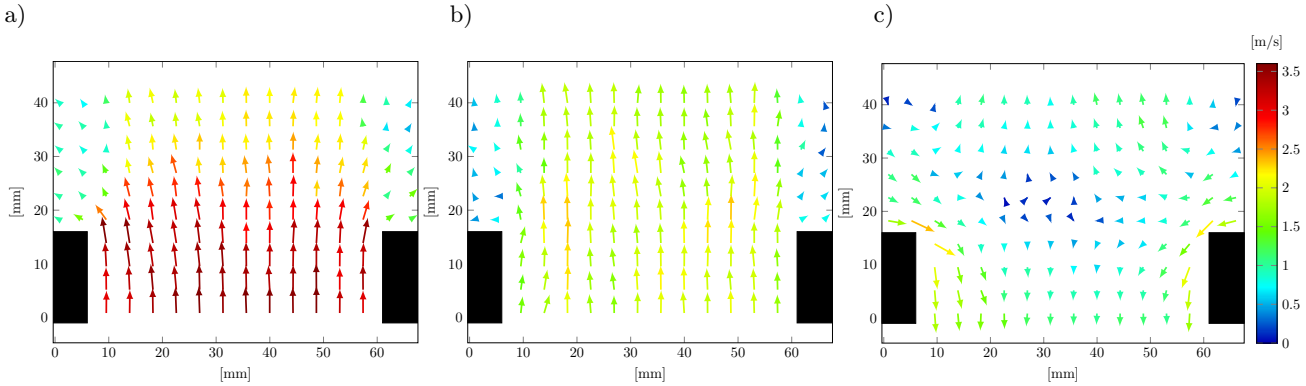

Fig. 6. Examples of the instantaneous velocity field at the pipe's open end: a) the instability maximum in the outward direction, b) an instant of vanishing instabilities (their turning point), c) the instability maximum in the inward direction. The color scale is kept the same in all panels but, for the sake of clarity, the arrows were enlarged by 50% in the middle and right panels.

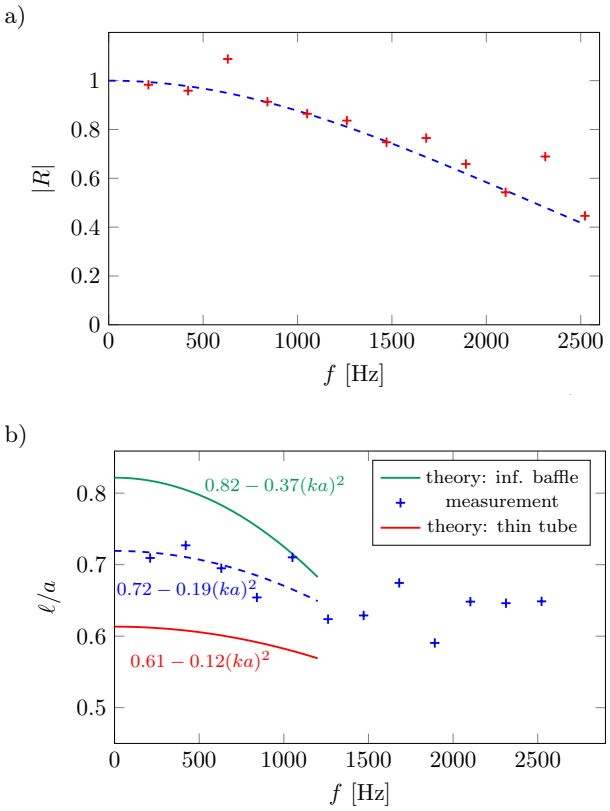

Fig. 7. a) Magnitudes of reflection coefficients. Experimental values as squares and the line is the theoretical prediction from Eq. (5). b) The end correction expressed as ℓ/a. The low Helmholtz number fit of the experimental data (blue, dashed) is compared to the theoretical predictions of Levine and Schwinger (1948) for infinitely thin tube and Nomura *et al.* (1960) for a tube in an infinite flange.

ℓ/a = 0.72 shall be put into consideration when dealing with wooden organ pipes. Ando (1969) gave the value ℓ/a = 0.69 for the wall thickness of 0.43a. Since our pipe has the wall thickness of approximately 0.54a, a slightly higher end correction appears to be in general accordance with the theoretical trends.

Although the results are in decent agreement with the theoretical predictions, note that this is an observation on a single case, so the specific value of the end correction shall be further tested to obtain a more reliable quantitative expression.

For the measured value of the Mach number, M = 0.005, corrections of the reflection coefficient and convected wave number should be very small. It implicates that even for the highest reasonable foot pressure, the effects of mean flow are tiny. In order to support this statement, the quality of the fit (Eq. (6)) was assessed by means of the coefficient of determination, r^2, for the convective as well as the not convected wavenumber (see Fig. 8). The fits are generally more precise for the convective case (however, the differences are tiny). In the same manner, the prediction of the reflection coefficient magnitude, according to Eq. (5) fits the data

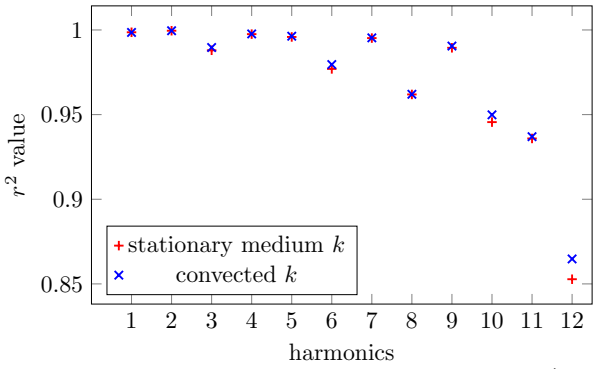

Fig. 8. Coefficient of determination values, r^2, for two differently formulated wavenumbers employed in Eq. (6).

slightly better for non-zero Mach number, but again, the differences are, in fact, negligible for our case.

To conclude, despite the fact that the flow profile resembling the fully developed turbulent pipe flow was experimentally confirmed and the flow separation occurs at the pipe's open end, the effects of these flow phenomena on the acoustic quantities are minimal.

5. Discussion

According to Munt's (1990) and Cargill's (1982) theory verified by experiments, there should be a maximum of the reflection coefficient magnitude exceeding 1 due to the flow-acoustic interactions in the perturbed free shear layer past the pipe's end. Such a phenomenon occurs even for low Mach numbers. The frequency at which this maximum should be observed corresponds to Sr ≈ π. For most organ pipes, such frequency is significantly lower than the fundamental (~27 Hz for our case), and therefore the sound quality is, very probably, not influenced by this effect. On the other hand, in principle, it might interact with some unwanted low-frequency instabilities occurring within the organ system.

The standing wave pressure obtained inside the pipe, as well as the amplitude of flow oscillations at the pipe's open end suggest that the sound pressure level in the pipe's interior exceeds 130 dB. However, among the observed effects there were not any that should be attributed to finite-amplitude wave steepening. It is fair to assume that the finite-amplitude nonlinearities are overcome by dissipative and dispersive effects in our case (see, e.g., (Hamilton *et al.*, 2008) for further commentary).

The misplaced value of the reflection coefficient magnitude on the 3rd harmonic (see Fig. 7) is a measurement error. The data are probably biased due to the proximity of the sound source partial and the broad resonance peak of the pipe eigenfrequency driven by the wideband noise of the turbulent motions inside the mouth (see the discussion in Fabre (2016)). In other

words, a slight detuning of the sound source frequency and the pipe eigenfrequencies plays the role here.

The impact of neglecting the difference between the upstream and downstream damping coefficient was tested as well. Making use of the expression by Ronneberger (1975) and retaining only the leading terms in the Mach number we arrive at the approximate relation $\alpha_-/\alpha_+ \approx 1+6.7\mathrm{M}$. For our pipe, it makes a difference of 3%. Given the generally low values of α_0 compared to k, this provides only "a correction to a correction" and the quality of the fit is unaffected. It means that the influence of the damping variation is less significant than the measurement uncertainties.

For the case of our experimental pipe, the difference between the traditional length correction $0.61a$ and the corrected value $0.72a$ presents a difference of 7 cents (i.e. close to the threshold value of the human perceptibility). Note, however, that under a reasonable change of the pipe scaling, this difference can exceed 10 cents easily, which makes it an influence to be considered. A real-world example of such a pipe is given in Fig. 9.

Fig. 9. A real-world example of an organ pipe for which the difference between length correction predictions $0.61a$ and $0.72a$ should be clearly audible.

Only the pressure reflection coefficient has been addressed throughout this article. Apart from it there is the energy reflection coefficient R_E, for which an additional Mach number dependence takes place (Hirschberg, Hoeijmakers, 2014):

$$R_E = \frac{(1-\mathrm{M})^2}{(1+\mathrm{M})^2}|R|^2 = (1-4\mathrm{M})|R|^2 + \mathcal{O}\left(\mathrm{M}^2\right). \qquad (8)$$

The last expression exhibits stronger dependence on the flow-acoustic features compared to the pressure reflection coefficient. However, it has not been experimentally tested in the course of this work.

6. Conclusions

It has been experimentally proven that there are cases in which the flow inside the flue organ pipe (but outside the mouth region) exhibits turbulent features, and the free jet is formed at the open end. However, interactions of the eddy viscosity with the acoustic boundary layer velocities are effectively excluded. Splitting the damping coefficient to the upstream and downstream parts appears to be unnecessary as well.

The influence of the low Mach number flow on the reflection coefficient is described by the Eq. (5) and it follows that such an effect might be neglected for a wide range of practical cases.

It has been pointed out that the wall thickness belongs among the primary factors governing the end correction. This feature was illustrated in a specific case, for which $\ell/a = 0.72$ was found, and compared with the theoretical predictions. It follows that the pipe wall thickness shall be considered as a contributor to the fine tuning of the organ pipes, especially the wooden ones.

Acknowledgements

This publication was written at the Academy of Performing Arts in Prague as part of the project "Subjective and objective aspects of musical sound quality" with the support of the Institutional Endowment for the Long Term Conceptual Development of Research Institutes, as provided by the Ministry of Education, Youth and Sports of the Czech Republic.

References

1. Ando Y. (1969), On the sound radiation from semi-infinite circular pipe of certain wall thickness, *Acta Acustica united with Acustica*, **22**(4): 219–225.
2. Blackstock D.T. (2000), *Fundamentals of Physical Acoustics*, Wiley & Sons, New York.
3. Cargill A. (1982), Low frequency acoustic radiation from a jet pipe – a second order theory, *Journal of Sound and Vibration*, **83**(3): 339–354, doi: 10.1016/S0022-460X(82)80097-7.
4. da Silva A.R., Greco G.F. (2019), Computational investigation of plane wave reflections at the open end of subsonic intakes, *Journal of Sound and Vibration*, **446**: 412–428, doi: 10.1016/j.jsv.2019.01.044.
5. da Silva A.R., Scavone G.P., Lenzi A. (2010), Numerical investigation of the mean flow effect on the acoustic reflection at the open end of clarinet-like instruments, *Acta Acustica united with Acustica*, **96**(5): 959–966.
6. Fabre B. (2016), Flute-like instruments, [in:] Chaigne A., Kergomard J., *Acoustics of Musical Instruments. Modern Acoustics and Signal Processing*, pp. 559–606, Springer: New York, NY, doi: 10.1007/978-1-4939-3679-3_10.
7. Fletcher N., Rossing T. (1998), *The Physics of Musical Instruments*, Springer: New York.
8. Hamilton M.F., Blackstock D.T. [Eds] (2008), *Nonlinear Acoustics*, Acoustical Society of America: Melville, NY.

9. Hirschberg A., Hoeijmakers M. (2014), Comments on the low frequency radiation impedance of a duct exhausting a hot gas, *The Journal of the Acoustical Society of America*, **136**(2): EL84–EL89, doi: 10.1121/1.4885540.
10. Hruška V., Dlask P. (2017), Connections between organ pipe noise and shannon entropy of the airflow: Preliminary results, *Acta Acustica united with Acustica*, **103**(6): 1100–1105, doi: 10.3813/AAA.919137.
11. Hruška V., Dlask P. (2019), Investigation of the sound source regions in open and closed organ pipes, *Archives of Acoustics*, **44**(3): 467–474, doi: 10.24425/aoa.2019.129262.
12. Hruška V., Dlask P., Guštar M. (2019), Nondestructive measurement of the pressure waveform and the reflectioncoefficient in a flue organ pipe, [in:] *Proceedings of the International Symposium on Music Acoustics 2019 – ISMA 2019*.
13. Jang S.-H., Ih J.-G. (1998), On the multiple microphone method for measuring in-duct acoustic properties in the presence of mean flow, *The Journal of the Acoustical Society of America*, **103**(3): 1520–1526, doi: 10.1121/1.421289.
14. Lautrup B. (2011), *Physics of Continuous Matter*, Taylor & Francis Inc.
15. Levine H., Schwinger J. (1948), On the radiation of sound from an unflanged circular pipe, *Physical Review*, **73**(4): 383–406, doi: 10.1103/PhysRev.73.383.
16. Mickiewicz W. (2015), Particle image velocimetry and proper orthogonal decomposition applied to aerodynamic sound source region visualization in organ flue pipe, *Archives of Acoustics*, **40**(4): 475–484, doi: 10.1515/aoa-2015-0047.
17. Munt R. (1990), Acoustic transmission properties of a jet pipe with subsonic jet flow: I. The cold jet reflection coefficient, *Journal of Sound and Vibration*, **142**(3): 413–436, doi: 10.1016/0022-460X(90)90659-N.
18. Nomura Y., Yamamura I., Inawashiro S. (1960), On the acoustic radiation from a flanged circular pipe, *Journal of the Physical Society of Japan*, **15**(3): 510–517, doi: 10.1143/JPSJ.15.510.
19. Peters M.C.A.M., Hirschberg A., Reijnen A.J., Wijnands A.P.J. (1993), Damping and reflection coefficient measurements for an open pipe at low mach and low helmholtz numbers, *Journal of Fluid Mechanics*, **256**: 499–534, doi: 10.1017/S0022112093002861.
20. Raffel M., Willert C.E., Wereley S.T., Kompenhans J. (2007), *Particle Image Velocimetry*. Springer: Berlin Heidelberg.
21. Rienstra S. (1983), A small strouhal number analysis for acoustic wave-jet flow-pipe interaction, *Journal of Sound and Vibration*, **86**(4): 539–556, doi: 10.1016/0022-460X(83)91019-2.
22. Ronneberger D. (1975), *Precise measurement of the sound attenuation and the phase velocity in pipes with a flow with regard to the interaction between sound and turbulence* [in German: *Genaue Messung der Schalldämpfung und der Phasengeschwindigkeit in durchströmten Rohren im Hinblick auf die Wechselwirkung zwischen Schall und Turbulenz*], Universität Göttingen.
23. Schlichting H., Gersten, K. (2016), *Boundary-Layer Theory*. Springer-Verlag GmbH.
24. Weng C., Boij S., Hanifi A. (2013), The attenuation of sound by turbulence in internal flows, *The Journal of the Acoustical Society of America*, **133**(6): 3764–3776, doi: 10.1121/1.4802894.
25. Yoshikawa S., Tashiro H., Sakamoto Y. (2012), Experimental examination of vortex-sound generation in an organ pipe: a proposal of jet vortex-layer formation model, *Journal of Sound and Vibration*, **331**(11): 2558–2577, doi: 10.1016/j.jsv.2012.01.026.